Journal of GeoEngineering, Vol. 17, No. 3, pp. 165-173, September 2022
http://dx.doi.org/10.6310/jog.202209_17(3).5

BI-DIRECTIONAL EFFECTS ON THE TUNNEL-SOIL-PILE INTERACTION UNDER SEISMIC LOADINGS

Md. Foisal Haque [1*]

ABSTRACT

The bi-directional mechanism influences tunnel forces and soil pressure when seismic excitation occurs. In this study, a tunnel-soil-pile interaction model was proposed, and an analytical formula was derived. These expressions consist of a bi-directional mechanism. In addition, the seismic excitation is considered as undamped free vibration, and the seismic wave shape is considered sinusoidal. Also, the soil behaves like an elastic, homogeneous, isotropic, and infinite medium to avoid the complexity of the formulation development. On the other hand, refractive and scattering waves and mode conversion of *P* or *SV* waves are not addressed in this study. Therefore, there is room to improve in the future. In parametric studies, the tunnel forces and soil pressure initially increased and then decreased after crossing a certain angle of incidence of seismic waves, according to bi-directionality. However, these synchronized behaviors were not seen for a single directional effect. In addition, the validation result of the bi-directional bending moment of the tunnel is nearly close. Therefore, it is essential to consider the bi-directionality in the interactive analysis.

Key words: Bi-directional effects, infinite medium, linear spring, seismic excitations, tunnel-soil-pile interaction.

1. INTRODUCTION

The bi-directional procedure addresses two approaches of seismic excitations, which have anti-plane of *SH* wave and in-plane of *SV* either *P* waves when the interaction system is affected by these waves. Several authors (Yih 2003; Meguid and Mattar 2009; Abdullah *et al.* 2013; Preeti and Jagan 2017; Deepankar *et al.* 2018) studied tunnel-soil-pile interaction for various loading conditions. Also, analytical formulae and numerical methods were developed by considering some parameters and assumptions, whereas tunnel forces and soil pressure of field observations were nearly close to these theoretical results. Tunnel forces have caused displacements, and piles have influenced the interactive tunnel force when soil is an interactive medium and acts as a linearly elastic spring. Ground movement is a vital issue during tunneling because it occurs during surface settlement, and disturbance of superstructure causes this settlement. Therefore, several authors (Lee *et al.* 1994; Coutts and Wang 2000; Tham and Deutscher 2000) evaluated tunneling-induced ground movements. Various numerical codes performed the numerical analysis, and evaluation of the bi-directional effect is possible from this analysis; however, some authors (Tabatabaiefar *et al.* 2013; Luan *et al.* 2015; Wen *et al.* 2017) have completed tunnel-soil-pile interaction by considering a single directional effect. That interaction represented behaviors of tunnel forces, soil pressure, and pile forces. In addition, it occurred when seismic shaking acted in the longitudinal direction of the tunnel. Several authors (Zhiming and Sanyuan 2008; Marshall and Haji 2014) developed analytical formulae based on Winkler's model and performed the finite element formulations in numerical analysis. The single directional wave effect also considered these conditions. The analytical formulations consist of some assumptions and do not include overall interaction behaviors. In some cases, results by using these formulae are nearly close to the numerical and field investigation results. Moreover, some authors (Chen *et al.* 1999; Kitiyodom *et al.* 2005; Lee *et al.* 2005; Cheng *et al.* 2007) predicted the variations of tunnel-soil-pile interaction results by using analytical, numerical, and field investigation procedures. The bi-directional effect of seismic excitation on the tunnel-soil-pile interaction system is uncertain. The single directional event of seismic excitation is a common problem, although in most cases this phenomenon has not occurred.

The model proposed in this study is designed for bi-directional seismic excitation, where the interacting system is simultaneously affected by the two types of anti-plane and in-plane seismic waves. However, the bi-directionality of the exciting wave is uncertain. The interactive analytical formulae of this model control the bi-directional mechanism. Therefore, to avoid complications, some assumptions are made for the materials such as homogeneity, isotropy, linear elasticity, and undamped infinite medium.

2. PROPOSED TUNNEL-SOIL-PILE INTERACTIVE MODEL FOR BI-DIRECTIONALITY

Two types of problems involve the bi-directional analysis as anti-plane and in-plane where the anti-plane *SH* wave incidence is reversed with either an in-plane *P* or *SV* wave. The *SH* waves also form an angle with the longitudinal axis of the tunnel shown in Fig. 1. One of the components of the anti-plane wave is equal to the in-plane waves. The tunnel, pile, and soil are divided into small parts according to the bi-directional analysis, and each small part contains all the characteristics required for the analytical formulations. Sever-

Manuscript received December 31, 2021; revised July 9, 2022; accepted July 10, 2022.
[1*] Ph.D. student (corresponding author), Department of Civil Engineering, Bangladesh University of Engineering and Technology, Dhaka-1000, Bangladesh (e-mail: mfh.civil@gmail.com).

al vertical elements (piles) stand parallel to the longitudinal axis of the tunnel, and the tunnel passes along the bodies to maintain spacing. To reduce the complexity of developing the analytical formula, the spacing of the front piles along the longitudinal direction of the tunnel was not considered. Also, the rear pile spacing is not considered for the same reason. These formulas, by applying a generalized equivalent technique, give a suitable effect of various magnitudes along the tunnel body. The diameters of piles are variable, and the distance between the tunnel and vertical element is also a changeable parameter, where the tunnel and this element connect a homogeneous, isotropic, elastic, and infinite soil medium. This medium acts as an equivalent linear spring. One of the simplified sinusoidal wave incidents at an angle with the longitudinal axis of the tunnel in the anti-plane of XY in Fig. 1. If it is an *SH* wave with no reflection observed on the tunnel body, any type of reflective wave is not included in the current formulations. To avoid complexity, the current formulation does not include reflected waves. Another reason is that after reflection (*P* or *SV* waves) on the tunnel body, its frequency gradually decreases or is absorbed by the surrounding soil. This is because the soil is considered a homogeneous medium in current formulations. Therefore, there is no possibility of further reflection or refraction on the soil body. At the same time as the *SH* wave, one of the in-plane sinusoidal waves (*P* or *SV*) incidents at an angle with the longitudinal direction of the tunnel at a similar location, which consists of the plane of XZ shown in Fig. 1.

This study was carried out in the frequency domain to avoid complex time-domain formulations, and the simplified seismic wave motion was a function of dimensionless frequency, where that frequency was the ratio of the incident wavelength to the characteristic wavelength. The incident wavelength depends on the characteristics and length of seismic waves. In addition, variations in tunnel forces and soil pressure control the wavelength variations. However, some assumptions in this study apply due to the reduced complexity of developing analytical formulations. Radiation damping or any damping of the materials is not addressed in this study. To confirm the effect of each material on seismic motion, it is necessary to predict the behavior of the structure under undamped conditions. In practice, all materials have specific damping properties.

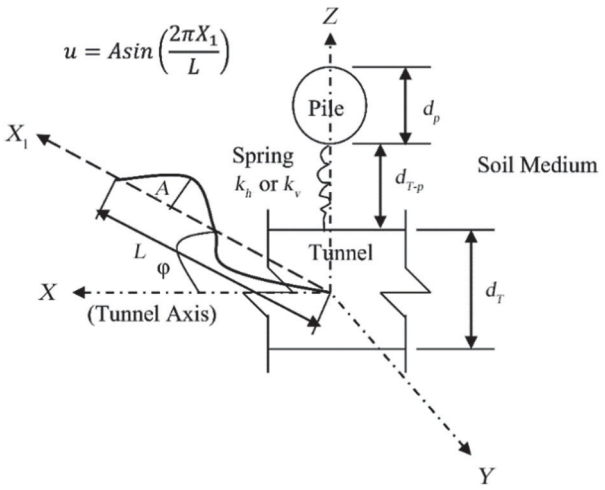

Fig. 1 Proposed tunnel-soil-pile interactive bi-directional model

3. BI-DIRECTIONAL FORMULAE OF PROPOSED TUNNEL-SOIL-PILE INTERACTIVE MODEL

The tunnel-soil-pile interactive model is affected by horizontal shear (*SH*), vertical shear (*SV*), and body (*P*) waves. Therefore, forces of tunnel and soil pressures are the function of incident angles, amplitudes, wavelengths, *etc.,* under various seismic loadings. Formulae are developed based on the undamped condition of simplified seismic wave-like sinusoidal waves, where a tunnel places the infinite soil medium for the development of formulations, which acts as a beam to connect by a series of piles with the linear elastic springs. So, the combined flexural rigidity of tunnel and vertical elements is affected by the present formulations. These formulations are free from the effect of the inertial forces of the tunnel as well as vertical elements. However, the forward propagating wave, which is a function of space and time, influences the combined curvature of the tunnel and pile. The bending moment, shear force, and soil pressure depend on this curvature.

3.1 Formulae of *SH* Wave

The horizontal shear (*SH*) wave acts at an angle with the longitudinal axis of the tunnel, and the in-plane wave has a presence in the system. So, two components influence this system, whether the curvature of the tunnel is the function of two anti-plane and in-plane components of the incident waves. These are the same in the X and Z directions components of the *SH* wave in Fig. 1. On the other hand, moment, shear, and soil pressure are the function of curvature. Vector representation of displacement of bi-directionality, derivation of curvature, and curvature for the moment have expressed the Eq. (1), Eqs. (2a) and (2b), respectively. The curvature of the tunnel is the function of the pile. It obtains partial differentiation of displacement under the space.

$$\{u_{SH}\}=\begin{Bmatrix} u_{x(SH)} \\ u_{y(SH)} \\ u_{z(SH)} \end{Bmatrix}=\begin{Bmatrix} A_{SH}\sin\varphi_{SH}\sin\left(\dfrac{2\pi X}{L_{SH}/\cos\varphi_{SH}}\right) \\ 0 \\ A_{SH}\cos\varphi_{SH}\sin\left(\dfrac{2\pi X}{L_{SH}/\cos\varphi_{SH}}\right) \end{Bmatrix} \tag{1}$$

$$\left\{1/\rho_{M(SH)}\right\}=\begin{Bmatrix} 1/\rho_{Mx(SH)} \\ 1/\rho_{My(SH)} \\ 1/\rho_{Mz(SH)} \end{Bmatrix}=\frac{\partial^2}{\partial x^2}\{u_{SH}\}=\frac{\partial^2}{\partial x^2}\begin{Bmatrix} u_{x(SH)} \\ u_{y(SH)} \\ u_{z(SH)} \end{Bmatrix} \tag{2a}$$

$$\left\{1/\rho_{M(SH)}\right\}=\begin{Bmatrix} 1/\rho_{Mx(SH)} \\ 0 \\ 1/\rho_{Mz(SH)} \end{Bmatrix}$$

$$= \begin{Bmatrix} -\left(\frac{2\pi}{L_{SH}}\right)^2 \sin\varphi_{SH} \cos^2\varphi_{SH} A_{SH} \sin\left(\frac{2\pi X}{L_{SH}/\cos\varphi_{SH}}\right) \\ 0 \\ -\left(\frac{2\pi}{L_{SH}}\right)^2 \cos^3\varphi_{SH} A_{SH} \sin\left(\frac{2\pi X}{L_{SH}/\cos\varphi_{SH}}\right) \end{Bmatrix} \quad (2b)$$

The elastic moduluis of tunnelling and piles are the same, but they differ from soil. The flexural rigidity is the function of the modulus of elasticity, the moment of inertia, and the distance between the tunnel and piles (Eq. (3)).

$$C_R = E_{T-P}\left\{I_T + \left(\sum_{f=1}^{k} I_{fP} + A_{fP} d_{f(T-P)}^2\right)\right\} \quad (3)$$

The interactive factor comes from the solution of the fourth-order generalized beam deflection equation. Formulae of this interaction system have been developed to consider the equivalent beam of the tunnel, which connects the piles by the linear elastic spring. This factor is the function of spring stiffness which comes from Kelvin's solution (John and Zahrah 1985), so the reduction factor is expressed by Eqs. (4a) and (4b).

$$\{R_{SH}\} = \{R_{x(SH)} \;\; R_{y(SH)} \;\; R_{z(SH)}\} = \{R_{x(SH)} \;\; 0 \;\; R_{z(SH)}\} \quad (4a)$$

$$\{R_{SH}\} = \begin{Bmatrix} \left(1+\frac{C_R}{k_{fh}}\left(\frac{2\pi}{L_{SH}}\right)^4 \cos^4\varphi_{SH}\right)^{-1} & 0 & \left(1+\frac{C_R}{k_{fh}}\left(\frac{2\pi}{L_{SH}}\right)^4 \cos^4\varphi_{SH}\right)^{-1} \end{Bmatrix} \quad (4b)$$

The interactive moment matrix comes from the multiplication of curvature, interactive factor, and flexural rigidity of the proposed model, as shown in Eq. (5a). The final form of the interactive bi-directional moment for the *SH* wave is given by Eq. (5b).

$$[M_{I(SH)}] = \{R_{SH}\}\{1/\rho_{M(SH)}\}C_R = \{R_{x(SH)} \;\; 0 \;\; R_{z(SH)}\}\begin{Bmatrix} 1/\rho_{Mx(SH)} \\ 0 \\ 1/\rho_{Mz(SH)} \end{Bmatrix} C_R \quad (5a)$$

$$[M_{I(SH)}] = [R_{x(SH)} C_R / \rho_{Mx(SH)} + R_{z(SH)} C_R / \rho_{Mz(SH)}] \quad (5b)$$

The interactive shear force matrix is the function of the interactive moment, and it comes from the partial differentiation of the interactive moment under the space as represented by Eq. (7), whether the derivative forms of shear force and curvature for the shear force express the Eqs. (6a) and (6b), respectively.

$$[V_{I(SH)}] = \frac{\partial}{\partial x}[M_{I(SH)}] \quad (6a)$$

$$\{1/\rho_{V(SH)}\} = \begin{Bmatrix} 1/\rho_{Vx(SH)} \\ 0 \\ 1/\rho_{Vz(SH)} \end{Bmatrix} = \begin{Bmatrix} -\left(\frac{2\pi}{L_{SH}}\right)^3 \sin\varphi_{SH} \cos^3\varphi_{SH} A_{SH} \cos\left(\frac{2\pi X}{L_{SH}/\cos\varphi_{SH}}\right) \\ 0 \\ -\left(\frac{2\pi}{L_{SH}}\right)^3 \cos^4\varphi_{SH} A_{SH} \cos\left(\frac{2\pi X}{L_{SH}/\cos\varphi_{SH}}\right) \end{Bmatrix} \quad (6b)$$

$$[V_{I(SH)}] = [R_{x(SH)} C_R / \rho_{Vx(SH)} + R_{z(SH)} C_R / \rho_{Vz(SH)}] \quad (7)$$

Similarly, the interactive soil pressure matrix finds the partial differentiation of interactive shear force shown in Eq. (9). In the same way as for interactive shear, the derivation forms of soil pressure and curvature for the soil pressure are given by Eqs. (8a) and (8b), respectively.

$$[P_{I(SH)}] = \frac{\partial}{\partial x}[V_{I(SH)}] \quad (8a)$$

$$\{1/\rho_{P(SH)}\} = \begin{Bmatrix} 1/\rho_{Px(SH)} \\ 0 \\ 1/\rho_{Pz(SH)} \end{Bmatrix} = \begin{Bmatrix} \left(\frac{2\pi}{L_{SH}}\right)^4 \sin\varphi_{SH} \cos^4\varphi_{SH} A_{SH} \sin\left(\frac{2\pi X}{L_{SH}/\cos\varphi_{SH}}\right) \\ 0 \\ \left(\frac{2\pi}{L_{SH}}\right)^4 \cos^5\varphi_{SH} A_{SH} \sin\left(\frac{2\pi X}{L_{SH}/\cos\varphi_{SH}}\right) \end{Bmatrix} \quad (8b)$$

$$[P_{I(SH)}] = [R_{x(SH)} C_R / \rho_{Px(SH)} + R_{z(SH)} C_R / \rho_{Pz(SH)}] \quad (9)$$

Horizontal spring stiffness is the function of the phase wave velocity. The characteristic length is given by Eq. (10). The phase wave velocity of the *SH* wave relates the Poisson's ratio of soil, tunnel diameter, and soil elastic modulus, and this stiffness comes from Kelvin's solution, which was described by John and Zahrah (John and Zahrah 1985).

$$k_{fh} = \frac{2\pi C}{L_{SH}} = \frac{2\pi}{L_{SH}} \frac{8G_S d_T (1-v_s)}{(3-4v_s)} \quad (10)$$

3.2 Formulae of *SV* Wave

The vertical shear (*SV*) wave propagates in the in-plane direction, and the *SH* wave acts as an anti-plane wave which is the same as the one component of the *SV* wave, so in this case, the incident angle contains two angular parts along the tunnel longitudinal and vertical directions. Therefore, vector representation of displacement of bi-directionality, double derivation of the vector forms displacement, and the moment-curvature are given by Eq. (11), Eqs. (12a), and (12b), respectively.

$$\{u_{SV}\}=\begin{Bmatrix}u_{x(SV)}\\u_{y(SV)}\\u_{z(SV)}\end{Bmatrix}=\begin{Bmatrix}A_{SV}\sin\varphi_{SV}\sin\left(\dfrac{2\pi X}{L_{SV}/\cos\varphi_{SV}}\right)\\A_{SV}\cos\varphi_{SV}\sin\left(\dfrac{2\pi X}{L_{SV}/\cos\varphi_{SV}}\right)\\0\end{Bmatrix} \tag{11}$$

$$\{1/\rho_{M(SV)}\}=\begin{Bmatrix}1/\rho_{Mx(SV)}\\1/\rho_{My(SV)}\\1/\rho_{Mz(SV)}\end{Bmatrix}=\frac{\partial^2}{\partial x^2}\{u_{SV}\}=\frac{\partial^2}{\partial x^2}\begin{Bmatrix}u_{x(SV)}\\u_{y(SV)}\\u_{z(SV)}\end{Bmatrix} \tag{12a}$$

$$\{1/\rho_{M(SV)}\}=\begin{Bmatrix}1/\rho_{Mx(SV)}\\1/\rho_{My(SV)}\\0\end{Bmatrix}=\begin{Bmatrix}-\left(\dfrac{2\pi}{L_{SV}}\right)^2\sin\varphi_{SV}\cos^2\varphi_{SV}A_{SV}\sin\left(\dfrac{2\pi X}{L_{SV}/\cos\varphi_{SV})}\right)\\-\left(\dfrac{2\pi}{L_{SV}}\right)^2\cos^3\varphi_{SV}A_{SV}\sin\left(\dfrac{2\pi X}{L_{SV}/\cos\varphi_{SV})}\right)\\0\end{Bmatrix} \tag{12b}$$

In this case, the reduction factor depends on the horizontal and vertical spring constants. Horizontal and vertical spring stiffnesses come from the solution of Kalvin and Flamant problems (John and Zahrah 1985). So this factor of *SV* wave a\is expressed as Eqs. (13a) and (13b). The vertical spring constant is related to the body (*P*) wave velocity and the characteristic length of the *SV* wave. Also, it is the function of the tunnel diameter as represented by Eq. (14).

$$\{R_{SV}\}=\{R_{x(SV)}\quad R_{y(SV)}\quad R_{z(SV)}\}=\{R_{x(SV)}\quad R_{y(SV)}\quad 0\} \tag{13a}$$

$$R_{SV}=\left\{\left(1+\frac{C_R}{k_{fh}}\left(\frac{2\pi}{L_{SV}}\right)^4\cos^4\varphi_{SV}\right)^{-1}\quad\left(1+\frac{C_R}{k_{fv}}\left(\frac{2\pi}{L_{SV}}\right)^4\cos^4\varphi_{SV}\right)^{-1}\quad 0\right\} \tag{13b}$$

$$k_{fv}=\frac{2\pi B}{L_{SV}}=\frac{2\pi}{L_{SV}}\frac{G_s d_T}{(1-v_s)}=\frac{2\pi}{L_{SV}}\frac{E_s d_T}{2(1+v_s)(1-v_s)} \tag{14}$$

The interactive moment matrix of the *SV* wave is the function of the curvature of the moment, reduction factor, and flexural rigidity, so the final mathematical form of this moment can be obtained from the multiplication of these functional parameters as expressed by Eqs. (15a) and (15b).

$$[M_{I(SV)}]=\{R_{SV}\}\{1/\rho_{M(SV)}\}C_R=\{R_{x(SV)}\quad R_{y(SV)}\quad 0\}\begin{Bmatrix}1/\rho_{Mx(SV)}\\1/\rho_{My(SV)}\\0\end{Bmatrix}C_R \tag{15a}$$

$$[M_{I(SV)}]=[R_{x(SV)}C_R/\rho_{Mx(SV)}+R_{y(SV)}C_R/\rho_{My(SV)}] \tag{15b}$$

The interactive shear force matrix of the *SV* wave is obtained by partial differentiation of interactive moment as shown in Eq. (16a), so the curvature for shear force and the final form of the interactive shear force matrix are represented by Eq. (16b) and Eq. (17).

$$[V_{I(SV)}]=\frac{\partial}{\partial x}[M_{I(SV)}] \tag{16a}$$

$$\{1/\rho_{V(SV)}\}=\begin{Bmatrix}1/\rho_{Vx(SV)}\\1/\rho_{Vy(SV)}\\0\end{Bmatrix}=\begin{Bmatrix}-\left(\dfrac{2\pi}{L_{SV}}\right)^3\sin\varphi_{SV}\cos^3\varphi_{SV}A_{SV}\cos\left(\dfrac{2\pi X}{L_{SV}/\cos\varphi_{SV})}\right)\\-\left(\dfrac{2\pi}{L_{SV}}\right)^2\cos^4\varphi_{SV}A_{SV}\cos\left(\dfrac{2\pi X}{L_{SV}/\cos\varphi_{SV})}\right)\\0\end{Bmatrix} \tag{16b}$$

$$[V_{I(SV)}]=[R_{x(SV)}C_R/\rho_{Vx(SV)}+R_{y(SV)}C_R/\rho_{Vy(SV)}] \tag{17}$$

An interactive soil pressure matrix finds the partial differentiation of the interactive shear force matrix under the space. The derivation form is given by Eq. (18a). The curvature for soil pressure and the final product of the interactive soil pressure matrix are given by Eq. (18b) and Eq. (19).

$$[P_{I(SV)}]=\frac{\partial}{\partial x}[V_{I(SV)}] \tag{18a}$$

$$\{1/\rho_{P(SV)}\}=\begin{Bmatrix}1/\rho_{Px(SV)}\\1/\rho_{Py(SV)}\\0\end{Bmatrix}=\begin{Bmatrix}\left(\dfrac{2\pi}{L_{SV}}\right)^4\sin\varphi_{SV}\cos^4\varphi_{SV}A_{SV}\sin\left(\dfrac{2\pi X}{L_{SV}/\cos\varphi_{SV})}\right)\\\left(\dfrac{2\pi}{L_{SV}}\right)^4\cos^5\varphi_{SV}A_{SV}\sin\left(\dfrac{2\pi X}{L_{SV}/\cos\varphi_{SV})}\right)\\0\end{Bmatrix} \tag{18b}$$

$$[P_{I(SV)}]=[R_{x(SV)}C_R/\rho_{Px(SV)}+R_{y(SV)}C_R/\rho_{Py(SV)}] \tag{19}$$

3.3 Formulae of *P* Wave

The body (*P*) wave propagates the in-plane direction at an angle with the longitudinal axis of the tunnel, and one of its

components is equal to the anti-plane *SH* wave. The vector representation of displacement due to the bi-directionality is expressed by Eq. (20). The curvature of the *P* wave finds the double differentiating of the final form of the equation of motion under the space, which is shown by Eq. (21a). Also, the final version of the curvature is given by Eq. (21b).

$$\{u_P\} = \begin{Bmatrix} u_{x(P)} \\ u_{y(P)} \\ u_{z(P)} \end{Bmatrix} = \begin{Bmatrix} A_P \cos\varphi_P \sin\left(\dfrac{2\pi X}{L_P / \cos\varphi_P}\right) \\ 0 \\ A_P \sin\varphi_P \sin\left(\dfrac{2\pi X}{L_P / \cos\varphi_P}\right) \end{Bmatrix} \tag{20}$$

$$\left\{1/\rho_{M(P)}\right\} = \begin{Bmatrix} 1/\rho_{Mx(P)} \\ 1/\rho_{My(P)} \\ 1/\rho_{Mz(P)} \end{Bmatrix} = \frac{\partial^2}{\partial x^2}\{u_P\} = \frac{\partial^2}{\partial x^2}\begin{Bmatrix} u_{x(P)} \\ u_{y(P)} \\ u_{z(P)} \end{Bmatrix} \tag{21a}$$

$$\left\{1/\rho_{M(P)}\right\} = \begin{Bmatrix} 1/\rho_{Mx(P)} \\ 0 \\ 1/\rho_{Mz(P)} \end{Bmatrix}$$

$$= \begin{Bmatrix} -\left(\dfrac{2\pi}{L_P}\right)^2 \cos^3\varphi_P A_P \sin\left(\dfrac{2\pi X}{L_P / \cos\varphi_P)}\right) \\ 0 \\ -\left(\dfrac{2\pi}{L_P}\right)^2 \sin\varphi_P \cos^2\varphi_P A_P \sin\left(\dfrac{2\pi X}{L_P / \cos\varphi_P)}\right) \end{Bmatrix} \tag{21b}$$

The tunnel considers a beam element for the derivation of the bi-directional formulations. The reduction factor of the body wave relates to the horizontal spring stiffness (Eq. (22a)), and the final form of the reduction factor for the *P* wave was obtained by solving the fourth-order generalized differential equation of beam, as shown by Eq. (22b).

$$\{R_P\} = \{R_{x(P)} \quad R_{y(P)} \quad R_{z(P)}\} = \{R_{x(P)} \quad 0 \quad R_{z(P)}\} \tag{22a}$$

$$R_P = \left\{\left(1 + \frac{C_R}{k_{fh}}\left(\frac{2\pi}{L_P}\right)^4 \cos^4\varphi_P\right)^{-1} \quad 0 \quad \left(1 + \frac{C_R}{k_{fh}}\left(\frac{2\pi}{L_P}\right)^4 \cos^4\varphi_P\right)^{-1}\right\} \tag{22b}$$

The interactive moment matrix of the *P* wave obtains the multiplication of the reduction factor, the curvature, and flexural rigidity, respectively (Eq. (23a)), and the final form of the interactive moment is given by Eq. (23b).

$$[M_{I(P)}] = \{R_P\}\{1/\rho_{M(P)}\} C_R$$

$$= \{R_{x(P)} \quad 0 \quad R_{z(P)}\}\begin{Bmatrix} 1/\rho_{Mx(P)} \\ 0 \\ 1/\rho_{Mz(P)} \end{Bmatrix} C_R \tag{23a}$$

$$[M_{I(P)}] = [R_{x(P)} C_R / \rho_{Mx(P)} + R_{z(P)} C_R / \rho_{Mz(P)}] \tag{23b}$$

The interactive shear force matrix is obtained by partial differentiating of the interactive moment matrix as shown in Eq. (24a), and the final form of the interactive shear force is expressed in Eq. (25), where the curvature for the shear force is given by Eq. (24b).

$$[V_{I(P)}] = \frac{\partial}{\partial x}[M_{I(P)}] \tag{24a}$$

$$\left\{1/\rho_{V(P)}\right\} = \begin{Bmatrix} 1/\rho_{Vx(P)} \\ 0 \\ 1/\rho_{Vz(P)} \end{Bmatrix}$$

$$= \begin{Bmatrix} -\left(\dfrac{2\pi}{L_P}\right)^3 \cos^4\varphi_P A_P \cos\left(\dfrac{2\pi X}{L_P / \cos\varphi_P)}\right) \\ 0 \\ -\left(\dfrac{2\pi}{L_P}\right)^3 \sin\varphi_P \cos^3\varphi_P A_P \cos\left(\dfrac{2\pi X}{L_P / \cos\varphi_P)}\right) \end{Bmatrix} \tag{24b}$$

$$[V_{I(P)}] = [R_{x(P)} C_R / \rho_{Vx(P)} + R_{z(P)} C_R / \rho_{Vz(P)}] \tag{25}$$

An interactive soil pressure matrix gets the partial differentiation of the interactive shear force matrix under the space, as shown by Eq. (26a). Also, the final form of this equation relates to the curvature. So, the curvature and final form of the soil pressure of the *P* wave can be expressed by Eq. (26b) and Eq. (27).

$$[P_{I(P)}] = \frac{\partial}{\partial x}[V_{I(P)}] \tag{26a}$$

$$\left\{1/\rho_{P(P)}\right\} = \begin{Bmatrix} 1/\rho_{Px(P)} \\ 0 \\ 1/\rho_{Pz(P)} \end{Bmatrix}$$

$$= \begin{Bmatrix} \left(\dfrac{2\pi}{L_P}\right)^4 \cos^5\varphi_P A_P \sin\left(\dfrac{2\pi X}{L_P / \cos\varphi_P)}\right) \\ 0 \\ \left(\dfrac{2\pi}{L_P}\right)^4 \sin\varphi_P \cos^4\varphi_P A_P \sin\left(\dfrac{2\pi X}{L_P / \cos\varphi_P)}\right) \end{Bmatrix} \tag{26b}$$

$$[P_{I(P)}] = [R_{x(P)} C_R / \rho_{Px(P)} + R_{z(P)} C_R / \rho_{Pz(P)}] \tag{27}$$

The interactive force matrixes are a function of the angle of incident, the amplitude of waves, the wavelength of waves, modulus of elasticities of soil, pile and tunnel, a moment of inertia of tunnel and vertical elements, *etc.*, The bi-directional formulations are developed based on the anti-plane consideration of the *SH* wave and the in-plane assumption of the *SV* or *P* waves.

4. PARAMETRIC STUDIES OF PROPOSED MODEL

An analytical formulation was developed to account for the bi-directionality of seismic waves. Parametric studies of the single and bi-directional effects of seismic excitations are carried out. Therefore, some necessary data are assumed for this study. The amplitude of the *SH* and *SV* waves is 100 mm, and the amplitude of the *P* wave is two-thirds that of the *SH* or *SV* waves. The length of *SH* and *SV* waves is the same, which is 12,500 mm. It is 25,000 mm for the *P* wave. For analysis, one-fourth of wavelength is assumed for analysis. The modulus of elasticities of the tunnel and piles are the same, but the soil is different. This value is 4,200 N/mm^2 for the tunnel and vertical element of the model. Also, it is 24 N/mm^2 for the surrounding medium. The diameters of the tunnel and pile are 11,800 mm and 500 mm, respectively. The distance between the tunnel body and pile face is 7,000 mm, which is constant. Poisson's ratio of soil was assumed to be 0.49.

4.1 Tunnel Moment

The interactive tunnel moment varies with the variations of various seismic wave incident angles. Initially, the magnitude of moments of *SH* and *SV* waves is low to consider the single and bi-direction. For *P* waves, the initial moment of single-direction is small but is high for the bi-direction. The interactive moment is maximum at an angle of 75° for *SH* and *SV* waves. In this location, the difference between the two methods is also the highest. Also, in this location, the interactive moment due to the bi-directional is almost five times higher than single direction considerations for *SH* and *SV* waves. The axial component of displacement is the main factor of variations between single and bi-directional results. The maximum moment indicates the worst condition or yielding of the tunnel structure. There are no result variations when the angle seems nearly zero and ninety degrees for *SH* and *SV* waves. For *P* waves, moment variation is similar to *SH* and *SV* waves based on both considerations. In addition, the moment is maximum at an angle of nearly 68° for single and bi-direction, while the bi-directional tunnel moment is 1.5 times higher than a single direction. Figure 2 represents interactive moment variations of *SH*, *SV*, and *P* waves.

4.2 Tunnel Shear Force

The tunnel shear gradually decreases with the increment of incident angles based on the single direction consideration for *SH* and *SV* waves. In bi-directionality, the shear force increases initially, then decreases gradually. Shear forces are maximum at an angle of nearly 70° based on bi-directionality for *SH* and *SV* waves. The bi-directional shear force is almost four times higher than the single direction consideration. For the *P* wave, the tunnel shear gradually increases with the increment of incident angles based on both cases. The shear force shows the maximum value at an angle of nearly 60° for the single direction. Also, it gives the maximum value at an angle of close to 55° for bi-directionality. In the *P* wave, the bi-directional shear of the tunnel is almost 1.5 times higher than the single direction consideration. So, the shear force of the tunnel is critical within the zone of 55° to 70°. The main reason for variations of results between single and bi-directionality is the axial component of

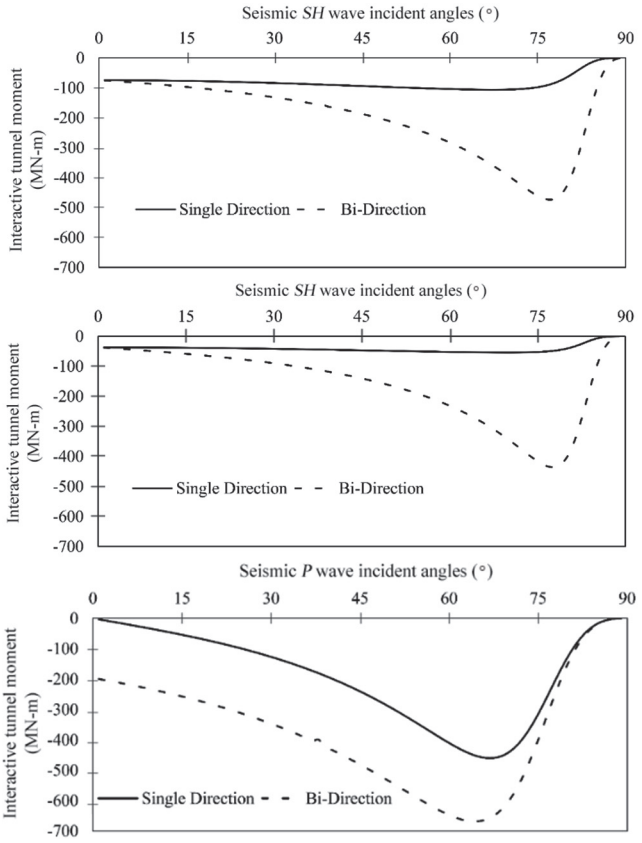

Fig. 2 Variations of interactive tunnel moments for various seismic waves

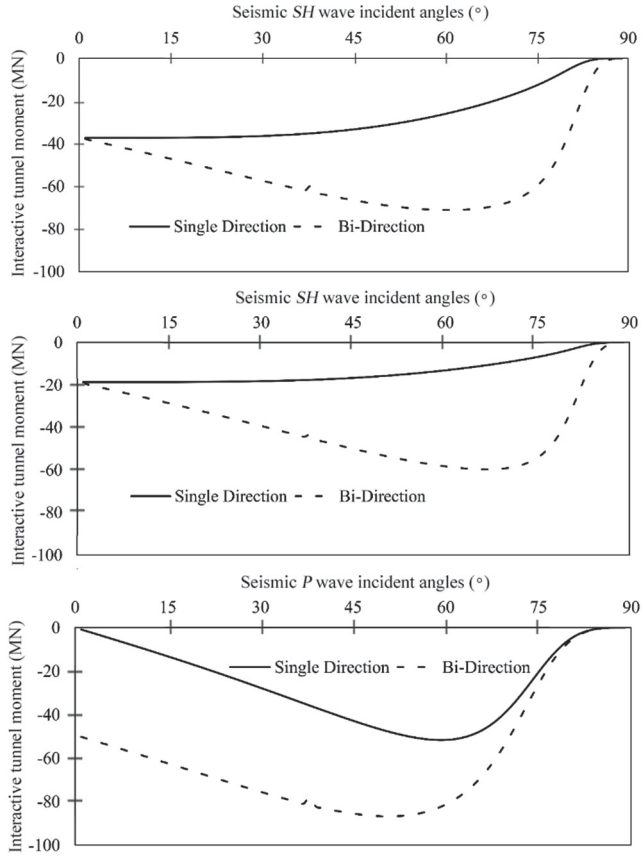

Fig. 3 Variations of interactive tunnel shears for various seismic waves

incident angles. Figure 3 expresses the tunnel shear variations of various seismic waves.

4.3 Soil Pressure

For bi-direction and *SH*, *SV*, and *P* waves, the interactive soil pressure increased initially and decreased after a certain level. The soil pressure decreased gradually based on the single direction consideration of *SH* and *SV* waves, and it becomes maximum when the angle becomes zero. Also, it has a minimum at angles close to ninety degrees. For the *P* wave, the maximum soil pressure was observed for the inclination of close to 50°, based on the single directional seismic excitation. An angle of almost 40° for bi-directionality is required for interactivity. The maximum interactive soil pressure difference between single and bi-directionality exhibits a gradient of nearly 45° for *SH* and *SV* waves. Figure 4 shows the variations of soil pressures for *SH*, *SV*, and *P* waves.

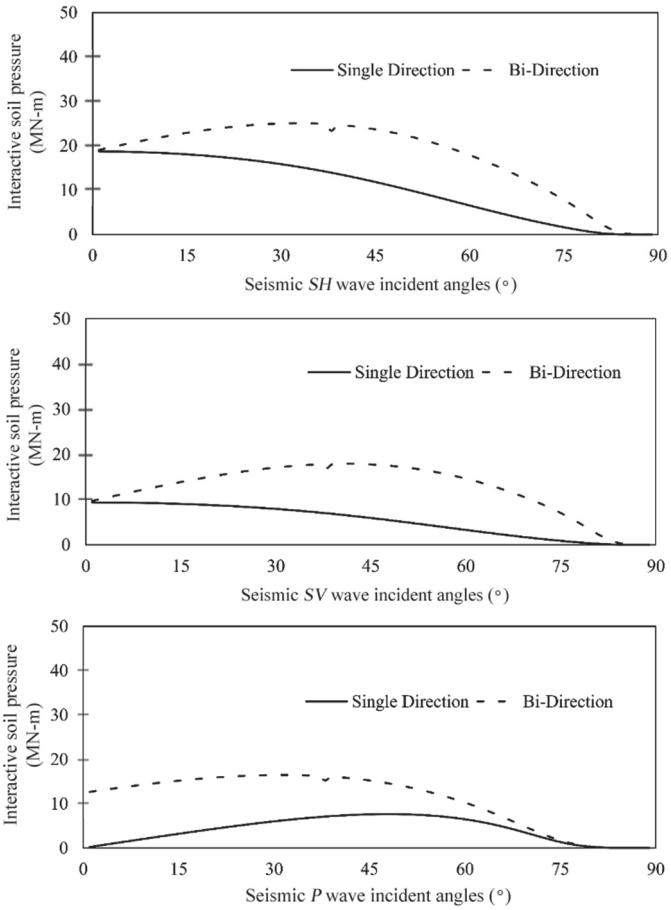

Fig. 4 Variations of interactive soil pressures for various seismic waves

5. VALIDATION OF PROPOSED MODEL BI-DIRECTIONAL FORMULAE

The bi-directional formulae of the present study validated the previous study (Lu *et al.* 2018), which was associated with Wang (1993), Penzien (2000), Bobet (2003), and Corigliano (2007). Therefore, the present research incorporates those analytical formulae results for more clarification. In that paper, numerical analysis was performed by Midas 2D and Midas 3D. The present study conducts the same analysis using analytical formulae of bi-directionality. More data are available in the previous research, but only necessary data were used for validation purposes. Depth of tunnel, the diameter of the tunnel, unit weight of soil, Poisson's ratio of soil, modulus of elasticity of soil, unit weight of tunnel lining material, Poisson's ratio of the tunnel, the thickness of tunnel lining, and modulus of elasticity of tunnel were found to be 50 m, 10 m, 20 kN/m^3, 0.25, 1.03 GPa, 25 kN/m^3, 0.25, 0.5 m and 38015 MN/m^2, respectively. The horizontal shear (*SH*) and body (*P*) waves acted along the transverse in the anti-plane direction and vertical axes in the in-plane direction of the tunnel. Validation results of *SH* and *P* waves are represented in Tables 1 and 2.

Table 1 Validation of bi-directional formulations for *SH* wave

Interactive tunnel force	Present study Eq. (5)	Previous studies results					
		Wang (1993)	Penzien (2000)	Bobet (2003)	Corigliano (2007)	MIDAS (2D)	MIDAS (3D)
Maximum bending moment (kN-m)	260.2	261.5	260.2	213.8	213.8	243.1	272.7

Table 2 Validation of bi-directional formulations for *P* wave

Interactive tunnel force	Present study Eq. (23)	Previous studies results			
		Bobet (2003)	Corigliano (2007)	MIDAS (2D)	MIDAS (3D)
Maximum bending moment (kN-m)	320.3	262.0	280.4	303.3	313.5

Validation results of *SH* and *P* waves are very close to each other. For the *SH* wave, the sequel of the present study decreases by 4.6% from the outcomes of Midas (3D). Similarly, this study result increases by 2.2% from the Midas (3D) solution.

6. CONCLUSIONS

The effect of bi-directionality controls tunnel forces and soil pressures. Also, variations of the results maintain a sequence without any types of fluctuations. The tunnel forces and soil pressures of bi-directional consideration are higher than the single direction due to the axial component of displacement. In addition, these forces and pressures have reached maximum values by maintaining a critical angle for most of the seismic waves based on both considerations. At the optimum angle, the stabilities of soil and tunnel reached the maximum level. When seismic waves acted perpendicular to the tunnel axis, the tunnel forces and soil pressures gave minimum values. The tunnel structural behaviors are affected by the material properties of soil and external seismic excitations. In practice, the transverse anti-plane component of the *SH* wave and the vertical in-plane part of the *SV* or *P* wave during seismic excitations disturbed the tunnel body and surrounding soil medium. The bi-directional formulae of the proposed model show the maximum behaviors of interactive systems such as tunnels, piles, and surrounding soil medium.

To avoid the complexity of developing the interaction formulations, the refractive, scattering, and mode conversion phenomena were not considered in the study. Therefore, there is room for future research to enhance this study by overcoming these limitations.

ACKNOWLEDGEMENTS

The author acknowledges reviewers, editors and supervisor for providing guidelines to complete this paper.

FUNDING

The author received no funding for this work.

DATA AVAILABILITY

All data and/or computer codes used/generated in this study are included in this paper.

CONFLICT OF INTEREST STATEMENT

There is no conflict of interest in this study.

NOMENCLATURE

A_{fp}	Cross sectional area of piles (m^2)
A_P	Displacement amplitude of body wave (mm)
A_{SH}	Displacement amplitude of transverse horizontal shear wave (mm)
A_{SV}	Displacement amplitude of vertical shear wave (mm)
B	Constant for vertical shear wave (kN/m)
C	Constant for transverse horizontal shear wave and body wave (kN/m)
$d_{f(T-P)}$	Linear distance between piles face and tunnel body face (mm)
d_P	Diameter of pile (mm)
d_T	Diameter of tunnel (mm)
E_{P-T}	Modulus of elasticity of piles or tunnel (N/mm^2)
E_s	Elastic modulus of soil (N/mm^2)
FE	Finite Element
G_s	Shear modulus of soil (N/mm^2)
I_{fP}	Centroidal axes moment of inertia of piles (m^4)
I_T	Centroidal axis moment of inertia of tunnel (m^4)
k	Maximum numerical number (-)
k_{fh}	Gross spring constant/stiffness of transverse horizontal shear wave and body wave (kN/m/m)
k_{fv}	Gross spring constant/stiffness of vertical shear wave (kN/m/m)
L_P	Wave length of body wave (mm)
L_{SH}	Wavelength of transverse horizontal shear wave (mm)
L_{SV}	Wave length of vertical shear wave (mm)
$M_{I(P)}$	Interactive bending moment of body wave (MN-m)
$M_{I(SH)}$	Interactive bending moment of transverse horizontal shear wave (MN-m)
$M_{I(SV)}$	Interactive bending moment of vertical shear wave (MN-m)
$P_{I(P)}$	Interactive soil pressure of body wave (MN/m)
$P_{I(SH)}$	Interactive soil pressure of transverse horizontal shear wave (MN/m)
$P_{I(SV)}$	Interactive soil pressure of vertical shear wave (MN/m)
R_P	Reduction factor of body wave (m)
R_{SH}	Reduction factor of transverse horizontal shear wave (m)
R_{SV}	Reduction factor of vertical shear wave (m)
$R_{x(P)}$	Reduction factor of body wave in X direction (m)
$R_{x(SH)}$	Reduction factor of transverse horizontal shear wave in X direction (m)
$R_{x(SV)}$	Reduction factor of vertical shear wave in X direction (m)
$R_{y(P)}$	Reduction factor of body wave in Y direction (m)
$R_{y(SH)}$	Reduction factor of transverse horizontal shear wave in Y direction (m)
$R_{y(SV)}$	Reduction factor of vertical shear wave in Y direction (m)
$R_{z(P)}$	Reduction factor of body wave in Z direction (m)
$R_{z(SH)}$	Reduction factor of transverse horizontal shear wave in Z direction (m)
$R_{z(SV)}$	Reduction factor of vertical shear wave in Z direction (m)
u_P	Total displacement of body wave (mm)
u_{SH}	Total displacement of transverse horizontal shear wave (mm)
u_{SV}	Total displacement of vertical shear wave (mm)
$u_{x(P)}$	Displacement of body wave in X direction (mm)
$u_{x(SH)}$	Displacement of horizontal shear wave in X direction (mm)
$u_{x(SV)}$	Displacement of vertical shear wave in X direction (mm)
$u_{y(P)}$	Displacement of body wave in Y direction (mm)
$u_{y(SH)}$	Displacement of horizontal shear wave in Y direction (mm)
$u_{y(SV)}$	Displacement of vertical shear wave in Y direction (mm)
$u_{z(P)}$	Displacement of body wave in Z direction (mm)
$u_{z(S)}$	Displacement of horizontal shear wave in Z direction (mm)
$u_{z(SV)}$	Displacement of vertical shear wave in Z direction (mm)
$V_{I(P)}$	Interactive shear force of body wave (MN)
$V_{I(SH)}$	Interactive shear force of transverse horizontal shear wave (MN)
$V_{I(SV)}$	Interactive shear force of vertical shear wave (MN)
X, Y, Z	Global axes
φ_{SH}	Angle of incident of transverse horizontal shear wave with the tunnel axis (°)
φ_{SV}	Angle of incident of vertical shear wave with the tunnel axis (°)
φ_P	Angle of incident of body wave with the tunnel axis (°)
$\rho_{M(P)}$	Radius of curvature for body wave (mm)
$\rho_{M(SH)}$	Radius of curvature for horizontal shear wave (mm)
$\rho_{M(SV)}$	Radius of curvature for vertical shear wave (mm)
$\rho_{Mx(P)}$	Radius of curvature for body wave in X direction (mm)
$\rho_{Mx(SH)}$	Radius of curvature for horizontal shear wave in X direction (mm)
$\rho_{Mx(SV)}$	Radius of curvature for vertical shear wave in X direction (mm)

$\rho_{My(P)}$ Radius of curvature for body wave in Y direction (mm)
$\rho_{My(SH)}$ Radius of curvature for horizontal shear wave in Y direction (mm)
$\rho_{My(SV)}$ Radius of curvature for vertical shear wave in Y direction (mm)
$\rho_{Mz(P)}$ Radius of curvature for body wave in Z direction (mm)
$\rho_{Mz(SH)}$ Radius of curvature for horizontal shear wave in Z direction (mm)
$\rho_{Mz(SV)}$ Radius of curvature for vertical shear wave in Z direction (mm)
υ_s Poisson's ratio of soil

REFERENCES

Abdullah, M.H. and Taha, M.R. (2013). "A review of the effects of tunneling on adjacent piles." *European Journal of Government and Economics, EJGE*, **18**, 2739-2762.

Bobet, A. (2003). "Effect of pore water pressure on tunnel support during static and seismic loading." *Tunneling and Underground Space Technology*, **18**, 377-393. https://doi.org/10.1016/S0886-7798(03)00008-7

Chen, L.T., Poulos, H.G., and Loganathan, N. (1999). "Pile responses caused by tunneling." *Journal of Geotechnical and Geoenvironmental Engineering*, ASCE, **125**(3), 207-215. https://doi.org/10.1061/(ASCE)1090-0241(1999)125:3(207)

Cheng, C.Y., Dasari, G.R., Chow, Y.K., and Leung, C.F. (2007). "Finite element analysis of tunnel-soil-pile interaction using displacement controlled model." *Tunnelling and Underground Space Technology*, **22**(4), 450-466. https://doi.org/10.1016/j.tust.2006.08.002

Corigliano, M. (2007). *Seismic Response of Rock Tunnels in Near-Fault Conditions*. Doctoral Dissertation, Politecnico di Torino.

Coutts, D.R. and Wang, J. (2000). *Monitoring of Reinforced Concrete Piles under Horizontal and Vertical Loads due to Tunneling*. 1st ed. s.l.: Taylor & Francis Group.

Deepankar, C., Patil, M., Patil, M., Ranjith, P.G. and Zhao, J. (2018). "Dynamic tunnel-soil interaction in soft soils considering site-specific seismic ground response." *Proceedings of the Indian Geotechnical Conference*, Bengaluru, India, 1-21.

John, C.M. and Zahrah, T.F. (1985). *Aseismic Design of Underground Structures*. National Science Foundation, Grant No. CEE-8310631. Report 8411-5616.

Kitiyodom, P., Matsumoto, T., and Kawaguchi, K. (2005). "A simplified analysis method for piled raft foundations subjected to ground movements induced by tunnelling." *International Journal for Numerical and Analytical Methods in Geomechanics*, **29**, 1485-1507. https://doi.org/10.1002/nag.469

Lee, G.T.K. and Ng, C.W.W. (2005). "Effects of advancing open face tunnelling on an existing loaded pile." *Journal of Geotechnical and Geoenvironmental Engineering*, ASCE, **131**(2), 193-201. https://doi.org/10.1016/(ASCE)1090-0241(2005)131:2(193)

Lee, R.G., Turner, A.J., and Whitworth, L.J. (1994). *Deformations Cased by Tunneling Beneath a Piled Structure*. London, University Press.

Lu, Q., Chen, S., Chang, Y., and He, C. (2018). "Comparison between numerical and analytical analysis on the dynamic behavior of circular tunnels." *Earth Science Research Journal*, **22**(2), 119-128. http://dx.doi.org/10.15446/esrj.v22n2.72248

Luan, L., Liu, Y., and Li, Y. (2015). "Numerical simulation for the soil-pile-structure interaction under seismic loading." *Mathematical Problems in Engineering*, **215**. https://doi.org/10.1155/2015/959581

Marshall, A.M. and Haji, T. (2014). "An analytical study of tunnel-pile interaction." *Tunneling and Underground Space Technology*, **45**, 43-51. https://doi.org/10.1016/j.tust.2014.09.001

Meguid, M.A. and Mattar, J. (2009). "Investigation of tunnel-soil-pile interaction in cohesive soils." *Journal of Geotechnical and Environmental Engineering*, ASCE, **135**(7), 973-979. https://doi.org/10.1061/(ASCE)GT.1943-5606.0000004

Penzien, J. (2000). "Seismically induced racking of tunnel linings." *Earthquake Engineering and Structural Dynamics*, **29**, 683-691. https://doi.org/10.1002/(SICI)1096-9845(200005)29:5<683::AID-EQE932>3.0.CO;2-1

Preeti, C. and Jagan, M.K. (2017). "Seismic analysis of soil-pile interaction under various soil condition." *International Journal of Applied Engineering Research*, **12**(18), 7566-7571.

Tabatabaiefar, H.R., Fatahi, B., and Samali, B. (2013). "Seismic behavior of building frames considering dynamic soil-structure interaction." *International Journal of Geomechanics*, ASCE, **13**(4), 409-420. https://doi.org/10.1061/(ASCE)GM.1943-5622.0000231

Tham, K.S. and Deutscher, M.S. (2000). "Tunnelling under woodleigh workers." *Quarters on Contract 705*. s.l.: Tunnels and Underground Structures.

Wang, J.N. (1993). *Seismic Design of Tunnels, A State-of-the-Art Approach*. Monograph 7 Parsons Brinckerhoff Quade and Douglas, Inc., New York.

Wen, B., Zhang, L., Niu, D., and Zhang, M. (2017). "Soil-structure-equipment interaction and influence factors in an underground electrical sub-station under seismic load." *Applied Science*, **7**(1044), 1-23. https://doi.org/10.3390/app7101044

Yih, C.C. (2003). *Finite Element Study of Tunnel-Soil-Pile Interaction*. Master Thesis, National University of Singapore. http://scholarbank.nus.edu.sg/handle/10635/14128

Zhiming, Q. and Sanyuan, S. (2008). "Dynamic interaction of soil-pile-structure under seismic action." *Proceedings of the 14th World Conference on Earthquake Engineering*, Beijing, China, 1-8.